Bundling of Actin Filaments by α-Actinin Depends on Its Molecular Length

Rudolf K. Meyer and Ueli Aebi

M. E. Müller-Institute for High Resolution Electron Microscopy at the Biocenter, University of Basel, CH-4056 Basel, Switzerland

Abstract. Cross-linking of actin filaments (F-actin) into bundles and networks was investigated with three different isoforms of the dumbbell-shaped α-actinin homodimer under identical reaction conditions. These were isolated from chicken gizzard smooth muscle, *Acanthamoeba*, and *Dictyostelium*, respectively. Examination in the electron microscope revealed that each isoform was able to cross-link F-actin into networks. In addition, F-actin bundles were obtained with chicken gizzard and *Acanthamoeba* α-actinin, but not *Dictyostelium* α-actinin under conditions where actin by itself polymerized into disperse filaments. This F-actin bundle formation critically depended on the proper molar ratio of α-actinin to actin, and hence F-actin bundles immediately disappeared when free α-actinin was withdrawn from the surrounding medium. The apparent dissociation constants (K_ds) at half-saturation of the actin binding sites were 0.4 μM at 22°C and 1.2 μM at 37°C for chicken gizzard, and 2.7 μM at 22°C for both *Acanthamoeba* and *Dictyostelium* α-actinin. Chicken gizzard and *Dictyostelium* α-actinin predominantly cross-linked actin filaments in an antiparallel fashion, whereas *Acanthamoeba* α-actinin cross-linked actin filaments prefer-entially in a parallel fashion. The average molecular length of free α-actinin was 37 nm for glycerol-sprayed/rotary metal-shadowed and 35 nm for negatively stained chicken gizzard; 46 and 44 nm, respectively, for *Acanthamoeba*; and 34 and 31 nm, respectively, for *Dictyostelium* α-actinin. In negatively stained preparations we also evaluated the average molecular length of α-actinin when bound to actin filaments: 36 nm for chicken gizzard and 35 nm for *Acanthamoeba* α-actinin, a molecular length roughly coinciding with the crossover repeat of the two-stranded F-actin helix (i.e, 36 nm), but only 28 nm for *Dictyostelium* α-actinin. Furthermore, the minimal spacing between cross-linking α-actinin molecules along actin filaments was close to 36 nm for both smooth muscle and *Acanthamoeba* α-actinin, but only 31 nm for *Dictyostelium* α-actinin. This observation suggests that the molecular length of the α-actinin homodimer may determine its spacing along the actin filament, and hence F-actin bundle formation may require "tight" (i.e., one molecule after the other) and "untwisted" (i.e., the long axis of the molecule being parallel to the actin filament axis) packing of α-actinin molecules along the actin filaments.

IN 1964 α-actinin was discovered as a protein extracted from striated muscle promoting contraction of actomyosin gels and increasing the viscosity of F-actin solutions in vitro (Ebashi et al., 1964). As more effective separation methods became available, its interaction with actin was more systematically investigated (Holmes et al., 1971; Goll et al., 1972). Accordingly, the largest increase in viscosity of a F-actin solution containing a given amount of α-actinin was observed at 0°C. Under these conditions the viscosity reached a maximum at an α-actinin to actin ratio yielding about one α-actinin dimer molecule bound per crossover repeat (i.e., 36 nm) of the actin helix. A much higher α-actinin to actin ratio was needed to yield the same amount of bound α-actinin in solutions kept at 37°C.

α-Actinin is a homodimer composed of two polypeptides of ∼100 kD each (Suzuki et al., 1976). Electron micrographs of shadowed α-actinin have revealed a dumbbell-shaped molecule with the two subunits being oriented antiparallel in a side-by-side association thus having a central dyad axis of symmetry (e.g., Pollard et al., 1986). Each polypeptide has a highly conserved actin binding site located near the NH₂-terminal of the polypeptide chain that on the molecule is located on the "knob-like" protrusion at the end of the rod (Mimura and Asano, 1987; Imamura et al., 1988; Blanchard et al., 1989). As a consequence, α-actinin cross-links F-actin by binding with each end to an actin filament (Podlubnaya et al., 1975).

Over the past few years many more α-actin isoforms have been isolated and characterized (Feramisco and Burridge, 1980; Burridge and Feramisco, 1981; Pollard, 1981; Condeelis and Vahey, 1982; Duhaiman and Bamburg, 1984; Schleicher et al., 1984), and broadly cross-reacting antibodies have been raised (Lazarides and Burridge, 1975). The α-actinin–actin interaction of most nonmuscle isoforms was

found to be Ca^{2+}-sensitive (Burridge and Feramisco, 1981; Pollard, 1981; Condeelis and Vahey, 1982; Duhaiman and Bamburg, 1984). Indeed, the primary structure of α-actinin revealed some sequence homology with calmodulin and spectrin, in particular within its conserved Ca^{2+}-binding motives in the form of EF-hands (Baron et al., 1987; Noegel et al., 1987; Blanchard et al., 1989).

Cross-linking of F-actin by α-actinin results in actin filament networks occasionally revealing near regularly spaced α-actinin cross-bridges along actin filaments (Podlubnaya et al., 1975; Jockusch and Isenberg, 1981). Furthermore, α-actinin-induced actin filament bundling has been reported by several authors (Podlubnaya et al., 1975; Condeelis and Vahey, 1982; Endo and Masaki, 1982; Burn et al., 1985). As yet, however, no consensus has been reached concerning the optimal conditions leading to F-actin bundle formation. Among the many conditions explored, low temperature (Endo and Masaki, 1982) and addition of specific lipids (Burn et al., 1985) have been reported to be essential for bundle formation.

Here we have compared several parameters under identical experimental conditions for three α-actinin isoforms, one isolated from chicken gizzard smooth muscle, one from *Acanthamoeba*, and one from *Dictyostelium*. Dissociation constants of all three isoforms have been evaluated by a centrifugation assay. In addition, we have systematically investigated the conditions causing α-actinin-induced F-actin bundling. The relative polarities of actin filaments cross-linked by α-actinin have been determined by three-dimensional (3-D) reconstruction of the individual filaments. The molecular length of free and bound α-actinin, and the longitudinal spacing of the α-actinin molecules bound along actin filaments have been evaluated from both negatively stained and metal-shadowed electron micrographs. A model of actin bundle formation has been developed to explain the molecular mechanism(s) underlying these results.

Materials and Methods

Materials

All chemicals were of reagent grade. Adenosine 5'-triphosphate (ATP, disodium salt, grade I), phalloidin, and N,N'-p-phenylenedimaleimide (PDM) were from Sigma Chemical Co. (St. Louis, MO). Glutaraldehyde was purchased from Electron Microscopy Sciences (Fort Washington, PA). Dithiobis-(succinimidylpropionate) (DSP),[1] dimethyl-3,3'-dithiobispropionimidate (DTBP), dimethyl adipimidate (DMA), dimethyl suberimidate (DMS), and the BCA protein assay reagent were from Pierce Chemical Co. (Rockford, IL). N,N-Dimethylformamide (DMF) was from Fluka AG (Buchs, Switzerland), and Sephadex G-25 from Pharmacia (Uppsala, Sweden).

Proteins

Isolation of chicken gizzard smooth muscle, *Acanthamoeba*, and *Dictyostelium* α-actinin have been described elsewhere (Feramisco and Burridge, 1980; Pollard, 1981; Schleicher et al., 1984). To allow for an optimal comparison, as the last step of the protein preparation all three isoforms were concentrated to 2–19 mg/ml by 30% ammonium sulphate precipitation, followed by dialysis against 20 mM Tris-HCl, 20 mM NaCl, 1 mM EDTA, 0.05% (wt/vol) NaN_3, pH 7.5. Protein concentrations were determined by the BCA protein assay. Rabbit muscle actin was prepared according to Millonig et al. (1988) and was used at a concentration of ∼1 mg/ml.

---

1. *Abbreviation used in this paper*: DSP, dithiobis-(succinimidylpropionate).

Determination of the Apparent α-Actinin-F-Actin Dissociation Constant (K_d)

α-Actinin and actin were mixed at the desired molar ratio in 200-μl polycarbonate centrifugation tubes and the volume adjusted to 40 μl with distilled water. To these mixtures 10 μl of 5× concentrated standard actin polymerization buffer was added to yield a final concentration of 2.5 mM imidazole, 2 mM $MgCl_2$, 150 mM KCl, 0.2 mM ATP, pH 7.5, unless stated otherwise. These mixtures were incubated for 1 h at the indicated temperature (either 22 or 37°C) before centrifugation at 20,000 g for 15 min. Pellet and supernatant were carefully separated, and the pellet was redissolved in 100 μl gel sample buffer while the supernatant was mixed with 50 μl of 2× concentrated gel sample buffer for SDS-PAGE. After SDS-PAGE and Coomassie blue staining, the relative amounts of protein in the different gel bands were quantitated by scanning them with a Camag TLC II scanner.

Chemical Fixation of α-Actinin-F-Actin Complexes

Aliquots of actin and α-actinin were mixed to yield a final concentration of 0.5 mg/ml actin and from 0.015 to 1.2 mg/ml α-actinin. A 50-μl aliquot was polymerized by addition of 5× concentrated polymerization buffer to yield a final concentration of 5 mM Na-borate, 2 mM $MgCl_2$, 150 mM KCl, 0.2 mM ATP, pH 8.5, by adjusting the final volume to 250 μl with distilled water. After incubation for 1 h at room temperature, phalloidin (0.5 mg/ml in distilled water) was added to reach a molar ratio of phalloidin to actin of 2:1. This mixture was incubated for another 30 min at room temperature before it was fixed with glutaraldehyde added to a final concentration of 0.25%. Electron microscopy of unfixed samples revealed no significant differences in the morphology of the α-actinin-F-actin complex by the increase in pH or by the addition of phalloidin.

To explore optimal fixation conditions for other cross-linking reagents, DSP, DTBP, DMA, and DMS were solubilized in DMF (i.e., at concentrations of 10–30 mg/ml) and added to the polymerized α-actinin-actin mixtures to yield a 10- to 100-fold molar excess over actin. After a 5-min incubation, the cross-linked material was either analyzed by SDS-PAGE or applied to a small (1-ml) column filled with 0.5 ml Sephadex G-25 equilibrated with actin polymerization buffer. Actin filament bundles and networks remaining on top of the column were washed with 1 ml actin polymerization buffer before being recovered in 50 μl polymerization buffer for electron microscopy (see below).

Electron Microscopy

5-μl aliquots of either fixed or unfixed α-actinin-F-actin incubation mixtures, prepared as described above, were adsorbed to glow-discharged carbon-coated collodion films on copper grids for 1 min. Some of the grids were washed with one to three drops of either distilled water or buffer. Excess liquid was drained with filter paper, and the grids were negatively stained by sequentially placing them on three drops of 0.75% uranyl formate for ∼10 s each. Excess liquid was drained with filter paper and finally by suction with a capillary applied to the edge of the grid which was then permitted to air dry (Buhle et al., 1985).

For glycerol spraying, a dilute solution of α-actinin (i.e., 0.5–1 μM) was mixed with glycerol to a final concentration of 33%. A 50-μl aliquot of this mixture was sprayed onto freshly cleaved mica which was then placed en face on the rotary table of a freeze-etch apparatus (BA 511 M; Balzers AE, FL-9496 Balzers, Fürstentum, Liechtenstein) and dried in vacuo at room temperature for at least 1 h. Finally, the dried samples were rotary-shadowed with platinum-carbon at an elevation angle of ∼5° (Fowler and Aebi, 1983).

All specimens were examined in a Philips EM 300 electron microscope operated at 80 kV. Micrographs were recorded on Kodak SO-163 electron image film at nominal magnifications of either 10,000× or 55,000×. Magnification calibration was performed according to Wrigley (1968) using negatively stained catalase crystals.

Determination of Actin Filament Polarity

Actin filament polarity was determined by 3-dimensional (3-D) reconstruction of individual actin filament stretches within α-actinin cross-linked filament pairs. For this purpose, two near parallel stretches within a pair of actin filaments cross-linked by at least two α-actinin molecules were digitized relative to the same coordinate system, and each digitized filament stretch saved as an individual file. Then a 150–200-nm-long filament segment was first straightened using the cross-correlation function of the filament computed with a suitable reference. To achieve this, two patches along the fila-

ment were aligned and averaged to provide a reference that was insensitive to the filament curvature. A peak search algorithm marked the highest correlation peaks approximately centered on the filament axis. Finally, a smooth spline function was fitted through the peak positions, and the image was reinterpolated along lines running perpendicular to the spline (Engel and Reichelt, 1989). The consecutive steps ultimately leading to a 3-D reconstruction of a 3-6 cross-over-repeat long straightened filament stretch have been described in detail elsewhere (Aebi et al., 1986). From the 3-D reconstruction an "axial projection" was computed by summing 20 equidistant sections spanning one actin subunit, i.e., 5.5 nm. The vorticity of the axial projection was used to evaluate the polarity of the actin filament relative to the coordinate system it was initially digitized. Accordingly, a filament pair revealing axial projections with the same vorticities meant that the two filaments had the same polarity, i.e., were parallel, whereas axial projections with opposite vorticities meant that the two filaments within a pair had opposite polarity, i.e., were antiparallel.

Measurement of Molecular Lengths

The length of the different dumbbell-shaped α-actinin isoforms was measured by projecting micrographs recorded at 55,000× nominal magnification to a final magnification of 550,000× (negatively stained specimens) or 275,000× (rotary-shadowed specimens). At least 60-100 measurements were included in each histogram to calculate mean length values. The length of α-actinin molecules cross-linking two adjacent actin filaments in a "near perpendicular" orientation (i.e., "ladder-like" configurations) was measured from the midline of one filament to that of the other one along the α-actinin molecule. Care was taken to include all molecules of a given area in the statistics. In rotary-shadowed specimens in particular, the shorter molecules were often more difficult to be discerned and would have biased the corresponding histogram when left out.

Results

Evaluation of the Apparent α-Actinin-F-Actin K_d by a Centrifugation Assay

α-Actinin-F-actin interactions were investigated with three different α-actinin isoforms, one extracted from chicken gizzard smooth muscle (Feramisco and Burridge, 1980), one from Acanthamoeba (Pollard, 1981), and one from Dictyostelium (Schleicher et al., 1984). To quantitate the amount of α-actinin bound to F-actin, a centrifugation assay was set up allowing for the separation of α-actinin-F-actin complexes from unbound protein (see Materials and Methods). Chicken gizzard α-actinin-actin mixtures were polymerized both at room temperature (22°C) and at 37°C, whereas Acanthamoeba and Dictyostelium α-actinin-actin mixtures were evaluated at room temperature only. Under the centrifugation conditions used (i.e., 20,000 g for 15 min) no significant amounts of either α-actinin or F-actin alone did pellet (Fig. 1 a). However, F-actin together with increasing amounts of α-actinin could be sedimented upon increasing the α-actinin to actin ratio in the polymerization mixture (Fig. 1 b).

As revealed in Fig. 2, the results of each experiment were expressed as the molar ratio of pelleted (i.e., bound) α-actinin to total actin and plotted versus the molar amount of α-actinin remaining in the supernatant (i.e., free). Within the experimentally tested ranges (α-actinin, 0.02-1.9 mg/ml; actin, 0.05-0.8 mg/ml), the results were the same for either the amount of α-actinin being varied with a fixed amount of actin or vice versa. All of the resulting binding curves were sigmoidal in shape with a near linear part in the middle and saturating near 0.07 (mol/mol), corresponding to one α-actinin dimer per 14 actin monomers (i.e., seven actin molecules per α-actinin binding site). The apparent K_ds were estimated at half-saturation of the actin binding sites to be 0.4

μM at 22°C and 1.2 μM at 37°C for chicken gizzard α-actinin, and 2.7 μM at 22°C for both Acanthamoeba and Dictyostelium α-actinin (see Table I).

Conditions for F-Actin Bundle and Network Formation

To investigate α-actinin-F-actin complexes by electron microscopy, different amounts of α-actinin and actin were mixed under polymerizing conditions (i.e., 2 mM $MgCl_2$ and 150 mM KCl), and negatively stained for electron microscopy. As illustrated in Fig. 3 a, with unwashed samples compact F-actin bundles were revealed with both chicken gizzard and Acanthamoeba α-actinin. In contrast, when the samples were washed with polymerization buffer or distilled water before negative staining, no F-actin bundles were observed, but F-actin networks were instead (Fig. 3 b). Contrary to earlier findings (Condeelis and Vahey, 1982), in our hands, Dictyostelium α-actinin was unable to bundle actin filaments at low (e.g., 2 mM) $MgCl_2$ concentrations, irrespective of whether or not the samples were washed with polymerization buffer before negative staining (see below).

For chicken gizzard α-actinin the conditions for F-actin bundle and network formation were more systematically explored. Accordingly, actin filament networks were only observed for molar ratios of α-actinin to actin below 1:60. Actin filament networks mixed with a few small but compact F-actin bundles were found for molar ratios ranging between 1:60 and 1:20. For molar ratios $\geq$1:20 predominantly compact F-actin bundles were found. This result documents the critical concentration dependence of the α-actinin-F-actin interaction, and it explains the observed sensitivity to washing steps (see above) that, by removing unbound α-actinin, shifts the equilibrium towards disintegration of the bundles. In time course experiments compact F-actin bundles appeared in <15 min after mixing α-actinin and actin at room temperature, provided protein ratios and concentrations were favorable for bundle formation (see above).

Electron Microscopy of Chemically Cross-linked α-Actinin-F-Actin Complexes

To stabilize α-actinin-F-actin bundles and networks for electron microscopy, several chemical fixation protocols were explored. To this end, chicken gizzard α-actinin-F-actin mixtures were incubated with cross-linking reagents and their efficiency assayed by SDS-PAGE. Accordingly, high molecular weight α-actinin-actin complexes were observed with DSP, PDM, and glutaraldehyde. For additional stabilization of the actin filaments, phalloidin (Cooper, 1987) was added to most preparations after polymerization was complete and before one of the covalent cross-linking reagents (see above) was added. Unbound protein and excess fixative were removed from the reaction mixture by "sieving" the rather large actin filament bundles and networks on a small Sephadex G-25 column. The cross-linked actin-α-actinin aggregates did not significantly enter the column and could therefore be recovered from the top of the column. Examination in the electron microscope revealed DSP as the fixative yielding the best stabilized and preserved α-actinin-F-actin bundles and networks when applied with a 100-fold molar excess over actin. Fig. 3 c reveals DSP-fixed and column-cleaned smooth muscle α-actinin-F-actin bundles. Most of them "open up" at their ends to yield ladder-like α-actinin-F-
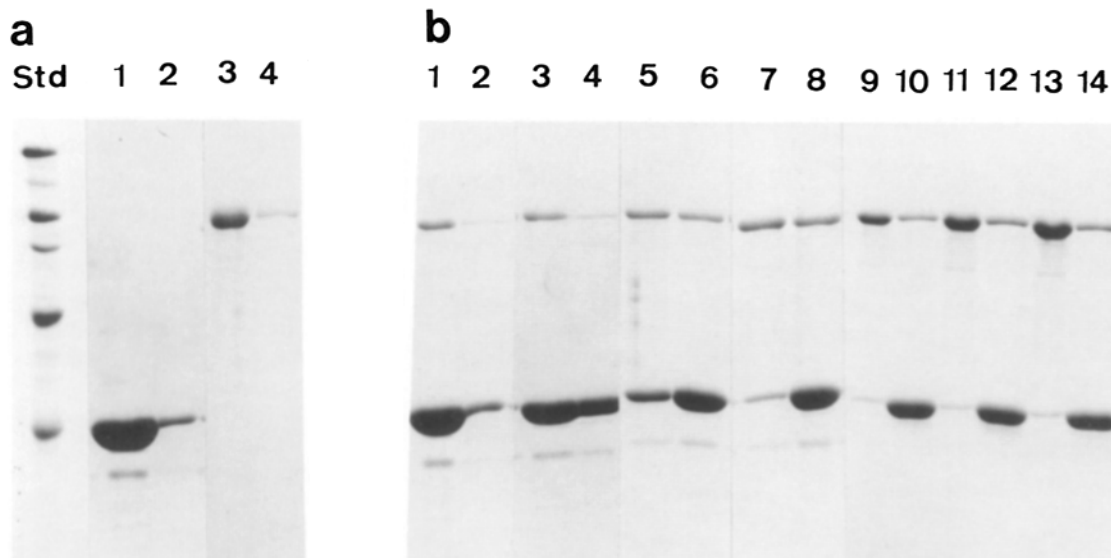
Figure 1. SDS-PAGE (8.5% gels) analysis of supernatants and pellets of α-actinin–F-actin mixtures. K_ds were determined by separation of bound from unbound α-actinin by centrifugation (for 15 min at 20,000 g) followed by quantitative gel analysis of supernatants (*odd numbered* lanes) and pellets (*even numbered* lanes). (*a*) Controls, 0.7 mg/ml actin (lanes *1* and *2*), and 0.5 mg/ml chicken gizzard α-actinin (lanes *3* and *4*). (*b*) Each sample contained either 0.7 (lanes *1-4*), or 0.5 mg/ml actin (lanes *5-14*) and, in addition, 0.025 (lanes *1* and *2*), 0.05 (lanes *3* and *4*), 0.1 (lanes *5* and *6*), 0.2 (lanes *7* and *8*), 0.3 (lanes *9* and *10*), 0.4 (lanes *11* and *12*), and 0.5 mg/ml (lanes *13* and *14*) chicken gizzard smooth muscle α-actinin. Each fraction was diluted 1:2 with sample buffer before a 10-μl aliquot was used for SDS-PAGE. Gel standards (*Std*): myosin, 200 kD; β-galactosidase, 116.25 kD; phosphorylase b, 97.4 kD; BSA, 66.2 kD; ovalbumin, 42.7 kD.

actin complexes with the cross-linking α-actinin molecules being oriented near perpendicularly along the actin filaments. In contrast, bundles of unfixed α-actinin–F-actin preparations (Fig. 3 *a*) do not open up at their ends, thereby concealing the geometrical arrangement of the α-actinin molecules relative to the actin filaments. Occasionally, ladder-like configurations are observed with unfixed samples if the α-acti-

Figure 2. Quantitative evaluation of the binding of α-actinin to F-actin. The amount of α-actinin bound to F-actin was determined by scanning the Coomassie blue–stained slab gels. The binding is expressed as the molar ratio of α-actinin dimer sedimented during centrifugation to total actin. In all cases, actin was polymerized in the presence of α-actinin. The sigmoidal binding curves saturate near 0.7 (mol/mol). Symbols: (*1*) chicken gizzard α-actinin at 22°C; (*2*) chicken gizzard α-actinin at 37°C; (*3*) *Acanthamoeba* α-actinin at 22°C; (*4*) *Dictyostelium* α-actinin at 22°C.

nin to actin ratio drops below the critical ratio for bundle formation (i.e., $\leqslant$1:20). As illustrated in Fig. 3 *d*, if the cross-linking step was omitted only few and disperse actin filaments with hardly any α-actinin molecules bound to them were recovered from the top of the column. In this case the actin bundles dissolved upon removing unbound α-actinin in the column cleaning step.

Higher magnification views of opened up, cross-linked and column-cleaned chicken gizzard α-actinin–F-actin bundles revealed a more detailed view of the ladder-like complexes with near perpendicularly oriented α-actinin molecules (Fig. 4 *a*). Accordingly, adjacent near parallel actin filaments were cross-linked at more or less regular intervals by α-actinin molecules arranged like the "rungs" of a ladder. Substitution of Mg^{2+} by Ca^{2+} did not alter the morphology, however as illustrated in Fig. 4 *b*, increasing the $MgCl_2$ concentration to 10 mM resulted in tighter packing of the actin filaments within the bundles and fewer opened up ends.

Acanthamoeba α-actinin–F-actin mixtures cross-linked by DSP and washed on a Sephadex G-25 column revealed actin bundles (Fig. 5 *b*) similar to those induced by chicken gizzard α-actinin (Fig. 5 *a*). However, already with 2 mM $MgCl_2$ the packing of the filaments within the bundles appeared somewhat tighter, and ladder-like α-actinin–F-actin complexes were more difficult to depict.

In contrast, no actin filament bundles were found in preparations containing *Dictyostelium* α-actinin under otherwise identical conditions both with and without DSP-cross-linking. As documented in Fig. 5 *c*, only actin filament networks sporadically cross-linked by α-actinin were observed despite the presence of 0.1 mM EGTA in the incubation mixtures to keep the Ca^{2+} ions below the concentration known to interfere with the *Dictyostelium* α-actinin–actin interaction (Con-
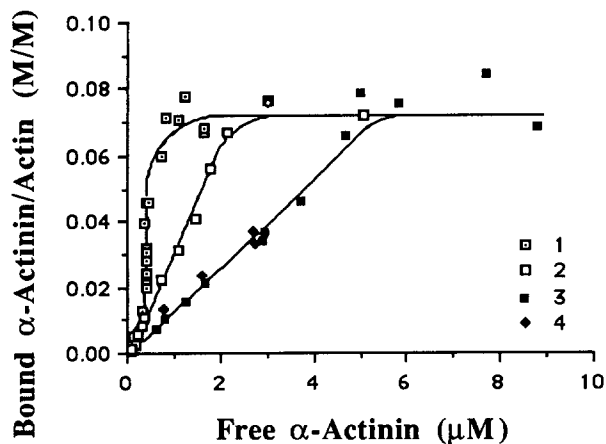
Table I. Characteristics of Chicken Gizzard Smooth Muscle, Acanthamoeba, and Dictyostelium α-Actinin Isoforms

Parameters	Chicken gizzard α-actinin	Acanthamoeba α-actinin	Dictyostelium α-actinin
Molecular length, free (rotary metal shadowed)	36.8 ± 3.1 nm	45.7 ± 6.1 nm	34.3 ± 4.5 nm
Molecular length, free (negatively stained)	34.8 ± 2.8 nm	44.1 ± 2.9 nm	31.4 ± 3.4 nm
Molecular length, bound to actin filaments (negatively stained)	36.1 ± 3.0 nm	35.0 ± 3.2 nm	28.1 ± 4.3 nm
Most frequent longitudinal spacings along actin filaments (negatively stained)	35–37 nm	35–37 nm	31–37 nm
K_d	0.4 μM* 1.2 μM‡	2.7 μM*	2.7 μM*
Orientation of cross-linked actin filaments	Antiparallel (9/11)§	Parallel (12/15)§	Antiparallel (7/10)§
Induces actin filament bundling	Yes	Yes	No

For all experiments, α-actinin and actin were mixed at the desired molar ratio before polymerization was induced by the addition of salt (see Materials and Methods).
* K_ds evaluated at 22°C.
‡ K_ds evaluated at 37°C.
§ Number of filament pairs showing the indicated polarity versus total number of filament pairs measured.

deelis and Vahey, 1982). Occasionally, α-actinin molecules could be depicted that cross-linked two adjacent actin filaments over a short stretch in a ladder-like configuration.

Relative Polarities of Actin Filaments Cross-linked by α-Actinin

To learn more about the α-actinin–F-actin interaction, we evaluated the relative polarities of actin filaments cross-linked by α-actinin molecules. Rather than determining actin filament polarity by myosin S-1 decoration (compare with Isenberg et al., 1980), we chose a more direct approach involving 3-D reconstruction of individual actin filament stretches within α-actinin cross-linked filament pairs. Accordingly, the handedness, and hence polarity, of the actin filaments could unequivocally be deduced from the vorticity of the axial projections computed from their 3-D reconstructions (see Materials and Methods). As illustrated in Fig. 6 (insets), depending on the relative orientation of the filaments, their axial projections exhibited either the same or opposite vorticities (see Materials and Methods). We therefore used this method to evaluate the relative polarities of actin filaments both in ladder-like α-actinin–F-actin complexes, as well as in F-actin networks cross-linked by α-actinin molecules for each of the three α-actinin isoforms. Loose networks were obtained by lowering the α-actinin to actin molar ratio below that required for bundle formation (i.e., below a ratio for which less than one α-actinin molecule per 200 actin molecules was effectively bound to the filaments; see Discussion). For electron microscopy, samples were stabilized by phalloidin and cross-linked by DSP as described in Materials and Methods, followed by washing on a Sephadex G-25 column, and negatively stained with uranyl formate (Fig. 6). Care was taken to only choose filament pairs for reconstruction which were crosslinked by at least two α-actinin molecules (Fig. 6, arrows). Actin fila-

ments cross-linked with chicken gizzard α-actinin revealed nine pairs with antiparallel and two pairs with parallel filament orientation, meaning that antiparallel cross-linking predominated. No significant difference was noticed between the relative orientation of adjacent actin filaments in bundles versus that in networks. With Dictyostelium α-actinin too, a preference for antiparallel cross-linking of adjacent actin filaments was observed, i.e., seven pairs out of 10 were antiparallel. In contrast, actin filaments cross-linked with Acanthamoeba α-actinin revealed 12 pairs out of 15 to be parallel, thus suggesting a preference for parallel cross-linking.

Molecular Length of the Different α-Actinin Isoforms

In was obviously neither the dissociation constant nor the relative polarities of cross-linked actin filaments which were responsible for the difference in F-actin bundling potential of chicken gizzard and Acanthamoeba α-actinin compared with that of Dictyostelium α-actinin. We therefore measured the length of free α-actinin molecules after glycerol spraying/rotary metal shadowing (Fig. 7, a–c). Mean lengths of 36.8 ± 3.1 nm for chicken gizzard, 45.7 ± 6.1 nm for Acanthamoeba, and 34.3 ± 4.5 nm for Dictyostelium α-actinin were obtained (Table I). With negatively stained preparations both the lengths of free α-actinin molecules (Fig. 7, d–f), as well as those of molecules bound to actin filaments (Fig. 7, g–i) were evaluated. The resulting histograms are presented in Fig. 8, a–c (solid lines, free molecules; dotted lines, bound molecules). Accordingly, the mean length of free chicken gizzard α-actinin was 34.8 ± 2.8 nm, while that of the bound molecules amounted to 36.1 ± 3.0 nm (Fig. 8 a and Table I), a statistically insignificant difference. In contrast, the mean length of free Acanthamoeba α-actinin was 44.1 ± 2.9 nm, whereas that of the bound molecules was significantly shorter, i.e., 35.0 ± 3.2 nm (Fig. 8 b and Table
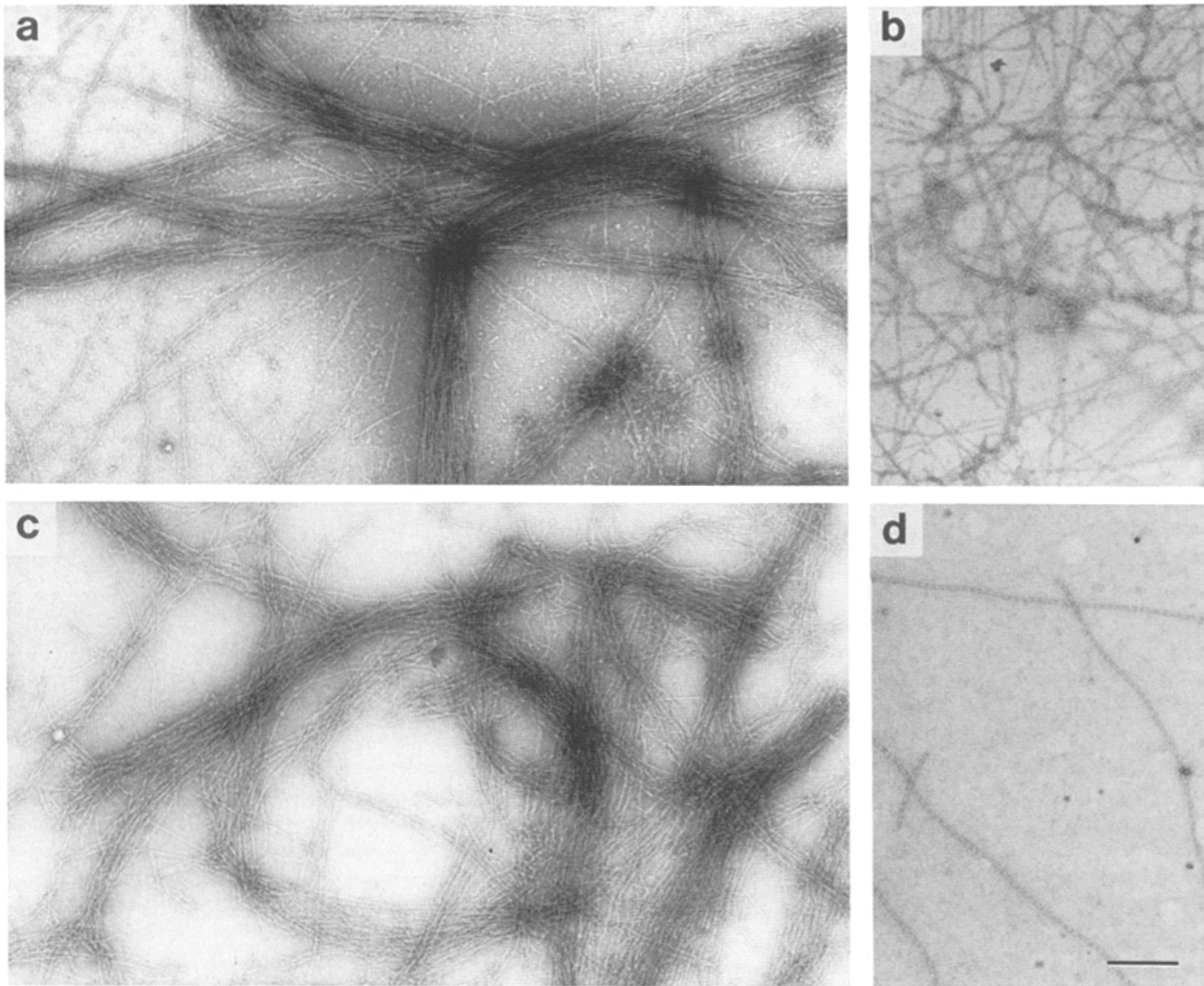
Figure 3. Stabilization of α-actinin–F-actin bundles by DSP fixation. (*a*) Bundles (unfixed) in an undiluted chicken gizzard α-actinin (0.32 mg/ml)–actin (0.5 mg/ml) mixture. (*b*) Same sample as in *a*, but in this case the free α-actinin pool was diluted by sequentially washing the grid on two drops of actin polymerization buffer followed by one drop of water before negative staining. As a consequence, the bundles opened up into networks. (*c*) Bundles polymerized in an α-actinin–actin mixture of similar composition as that in *a*, DSP fixed, and column cleaned. The bundles are essentially free of unbound proteins. (*d*) Only a few actin filaments could be recovered from the top of the cleaning column when DSP fixation was omitted but the sample otherwise prepared and treated as in *c*. All samples were negatively stained with 0.75% uranyl formate. Bar, 500 nm.

I). Finally, the mean length of free *Dictyostelium* α-actinin molecules was 31.4 ± 3.4 nm, and that of bound molecules 28.1 ± 4.3 nm (Fig. 8 *c* and Table I).

Longitudinal Spacing of the α-Actinin Molecules along Actin Filaments

We also measured the longitudinal (or axial) spacings between adjacent α-actinin molecules within ladder-like α-actinin–F-actin complexes in negatively stained preparations, e.g., as shown in Figs. 4 *a* and 7, *g–i*. Only distances were included in the histograms which were ≤72 nm (i.e., shorter than two times the length of an α-actinin molecule). As documented in Fig. 8, *d* and *e* for both chicken gizzard and *Acanthamoeba* α-actinin molecules a distinct peak of longitudinal spacings between 35 and 37 nm was revealed. In

contrast, *Dictyostelium* α-actinin gave a different, much broader peak between 31 and 37 nm (Fig. 8 *f*). The lower limits of these peaks, i.e., 35 nm for smooth muscle and *Acanthamoeba* α-actinin, and 31 nm for *Dictyostelium* α-actinin, roughly coincided with the mean length of the bound molecules for all three α-actinin isoforms (see the mean lengths ± SD marks drawn into the histograms representing the longitudinal spacings in Fig. 8, *d–f*). Accordingly, <25% of the measured longitudinal spacings were smaller than the mean length of the respective bound α-actinin molecules (24.7% for chicken gizzard, 8.7% for *Acanthamoeba*, and 17.0% for *Dictyostelium* α-actinin). The longitudinal spacings of the two isoforms exhibiting significant F-actin bundling potential (i.e., chicken gizzard and *Acanthamoeba* α-actinin) repeated roughly symmetrically relative to the
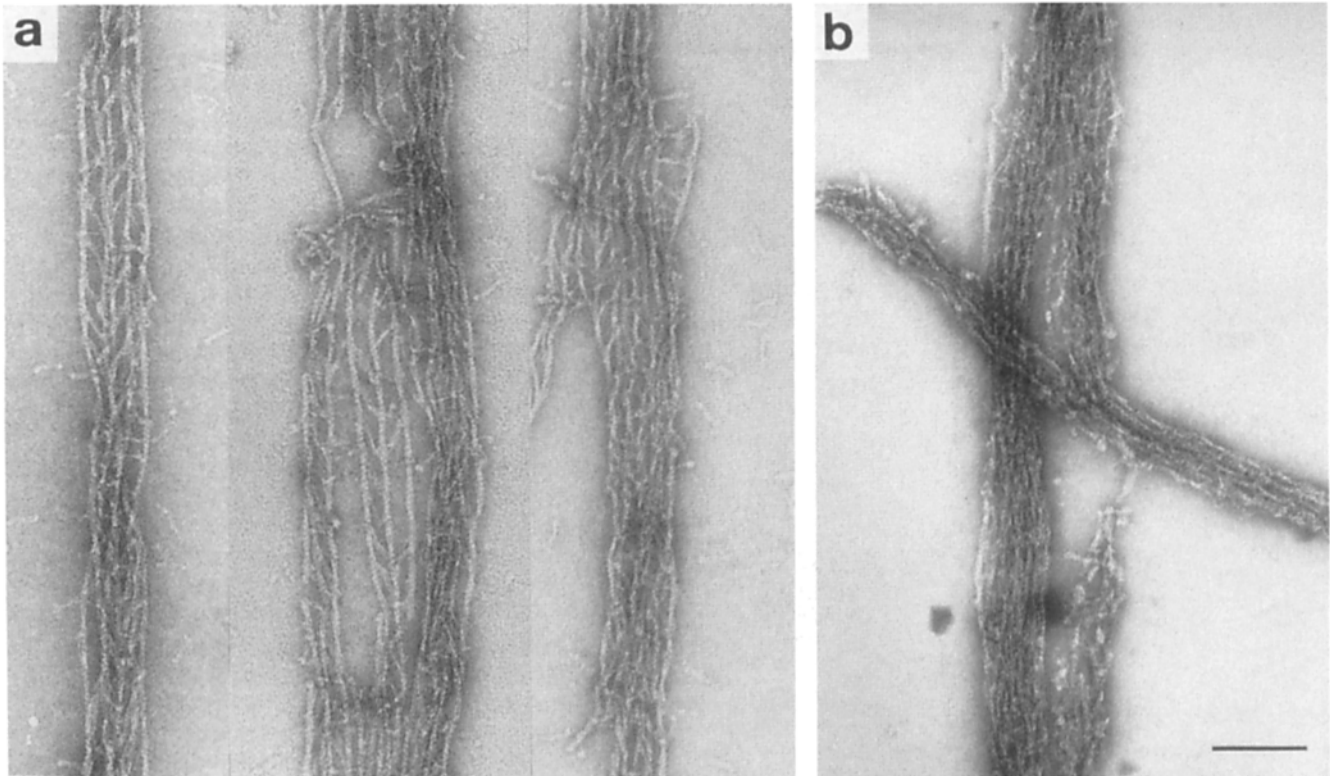
Figure 4. DSP-fixed and column-cleaned chicken gizzard α-actinin–F-actin (molar ratio 1:2.8) bundles formed with different Mg^{2+} concentrations. (*a*) With 2 mM $MgCl_2$, predominantly ladder-like complexes form in which the α-actinin molecules are arranged like the rungs of a ladder. (*b*) Increasing the Mg^{2+} concentration to 10 mM reveals increasingly more compact bundles. Samples have been negatively stained with 0.75% uranyl formate. Bar, 100 nm.
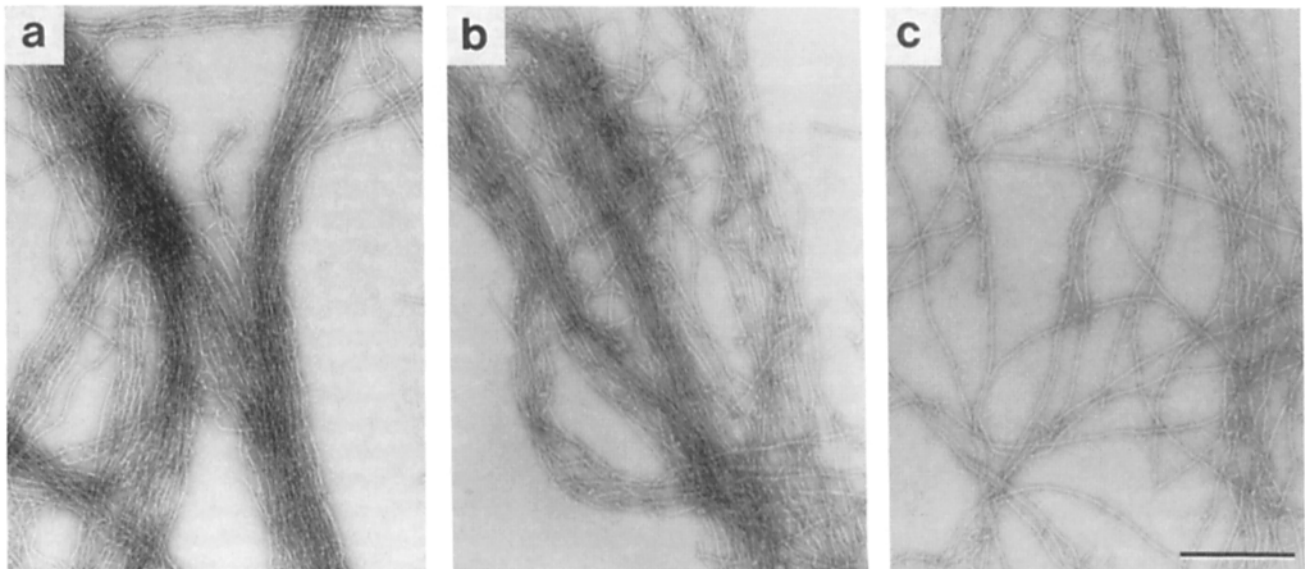

Figure 5. DSP-fixed and column-cleaned α-actinin–F-actin complexes cross-linked with different α-actinin isoforms. (*a*) Chicken gizzard (α-actinin to actin molar ratio, 1:2.8) and (*b*) *Acanthamoeba* (α-actinin to actin molar ratio, 1:2.3) α-actinin yield similar looking actin filament bundles. (*c*) Actin filament networks are formed with the much shorter *Dictyostelium* α-actinin (α-actinin to actin molar ratio, 1:1.7) under otherwise identical induction conditions. Samples have been negatively stained with 0.75% uranyl formate. Bar, 500 nm.
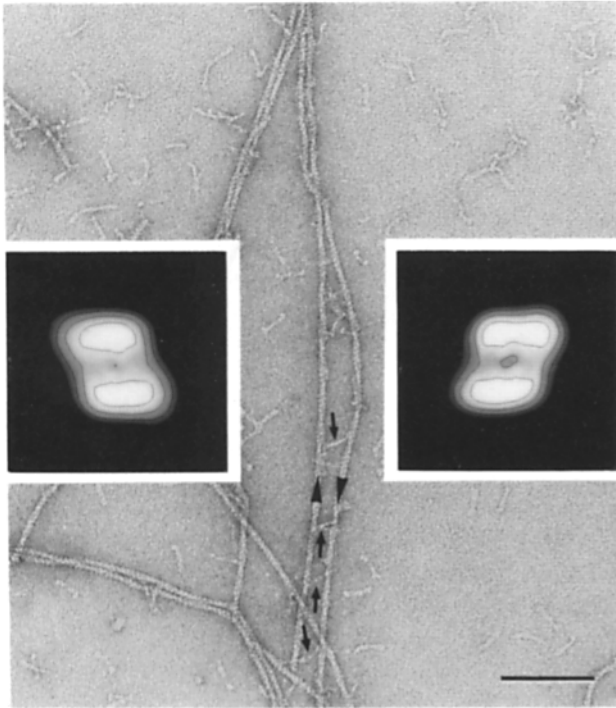
Figure 6. Determination of the relative polarity of adjacent actin filaments within α-actinin–F-actin bundles and networks. A pair of near parallel actin filaments cross-linked by several *Dictyostelium* α-actinin molecules (*arrows*) is shown. The two axial projections (*insets*) reveal opposite polarities of the two actin filaments within a pair (*arrowheads*). Samples have been negatively stained with 0.75% uranyl formate. Bar, 100 nm.

crossover distances of the F-actin helix (i.e., 35.8 nm), whereas those of *Dictyostelium* α-actinin did not.

Discussion

Apparent α-Actinin–F-Actin Dissociation Constants

The apparent K_ds of all three α-actinin isoforms studied are temperature dependent, with lower temperature resulting in tighter binding. At room temperature the K_d of chicken gizzard α-actinin is almost seven times lower than that measured for the two protozoan α-actinin isoforms. As a comparison, the binding affinity (i.e., at 22°C) of chicken gizzard α-actinin for actin is about half that of adducin, for example, which, in turn is considered a high affinity actin binding protein (Mische et al., 1987).

No matter how high an excess of α-actinin was added to a given amount of actin, saturation of the binding reaction always occurred at a molar ratio of 1 α-actinin dimer per 13–14 actin monomers, i.e., amounting to ∼1 α-actinin molecule per F-actin helical repeat (35.7 nm). This value agrees quite well with that deduced from direct measurement of the average minimal longitudinal spacing of α-actinin molecules bound along actin filaments in ladder-like configurations (Table I, and see below), as well as with published data (Holmes et al., 1971; Goll et al., 1972). We also added chicken gizzard α-actinin to preformed actin filaments and incubated the mixture for 1 h at 22°C. In this case, a K_d of

1.5 μM was revealed (data not shown), compared with 0.4 μM with copolymerization (Table I). While we have no explanation for this difference, it is consistent with a lower viscosity observed upon addition of a given amount of α-actinin to preformed actin filaments relative to that obtained upon polymerization of actin in the presence of the same amount of α-actinin under otherwise identical conditions (Goll et al., 1972).

Inspection in the electron microscope revealed that at saturation, for all three isoforms, a significant number of α-actinin molecules were only bound to one actin filament, i.e., one actin binding site per molecule was vacant. This might have been one of the reasons for the large scatter of values at saturation which, in turn, prevented accurate Scatchard analysis of the data.

Previously, a K_d of 26 μM was reported for *Acanthamoeba* α-actinin (Sato et al., 1987), a value roughly 10 times larger than that measured by us (i.e., 2.7 μM; Table I). However, in that investigation only 1.6 μM α-actinin was tested as the highest concentration for the binding assay, a value well below saturation for the actin concentrations (5–180 μM) used. According to our binding curve (Fig. 2), at least 5 μM *Acanthamoeba* α-actinin would have to be used with an actin concentration of 5 μM to reach saturation. K_ds are difficult to extrapolate if saturation is not accurately determined and, as a consequence, large errors may result (Light, 1984). To circumvent this problem, we have used up to 9.6 μM *Acanthamoeba* α-actinin with an actin concentration of 1 μM, an amount well above saturation.

According to our measurements (Table I), *Acanthamoeba* α-actinin, which bundles F-actin, and *Dictyostelium* α-actinin, which does not, have practically the same K_d. This finding argues against a primary involvement of the α-actinin–F-actin dissociation constant in defining the F-actin bundling potential.

α-Actinin-induced F-Actin Bundling

Actin filament bundles formed within minutes both with chicken gizzard and *Acanthamoeba* α-actinin–actin mixtures, provided buffer conditions were adequate for actin polymerization, and a critical α-actinin to actin molar ratio (∼1:20 for chicken gizzard α-actinin at 22°C) was exceeded. The minimal amount of α-actinin which is effectively bound at the critical molar ratio mentioned above can be evaluated from the measurements presented in Fig. 2 and amounts to one α-actinin molecule per ∼200 actin monomers. The exact amount of actin-bound α-actinin critically depends on the amount of free α-actinin, meaning that bundles disintegrate within seconds upon removing, or diluting out, the free α-actinin, as, for example, happens during routine washing of unfixed samples when prepared for electron microscopy. This behavior, in turn, may explain the fact that some investigators have apparently failed to detect α-actinin-induced F-actin bundles under conditions that should actually have been favorable for bundle formation (Jockusch and Isenberg, 1981; Endo and Masaki, 1982). Furthermore, the fact that actin bundles are more resistant to dissociation at lower temperature may have been the reason that Endo and Masaki (1982) only observed bundle formation at 0°C for both rabbit striated muscle and chicken gizzard smooth muscle α-actinin–F-actin mixtures.
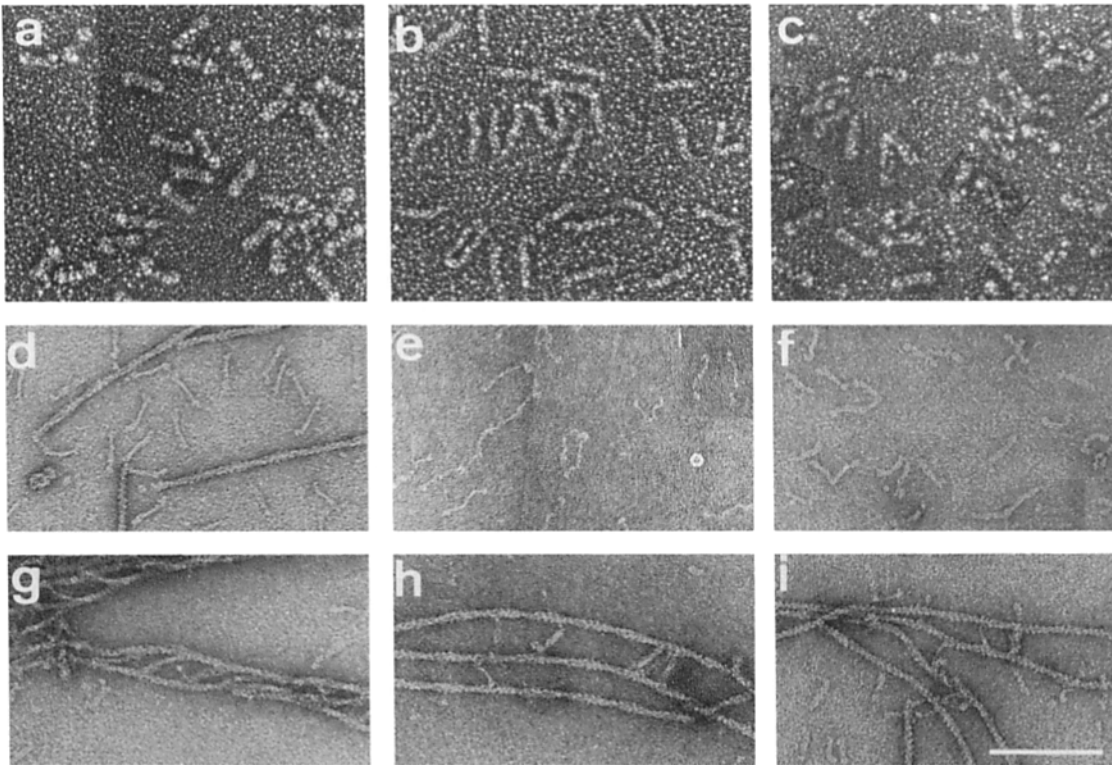
Figure 7. Electron micrographs of glycerol-sprayed/rotary metal-shadowed (*a–c*), and of negatively stained free (*a–f*) and F-actin-bound (*g–i*) α-actinin molecules. (*a, d,* and *g*) Chicken gizzard, (*b, e,* and *h*) *Acanthamoeba*, (*c, f,* and *i*) *Dictyostelium* α-actinin. Bar, 100 nm.
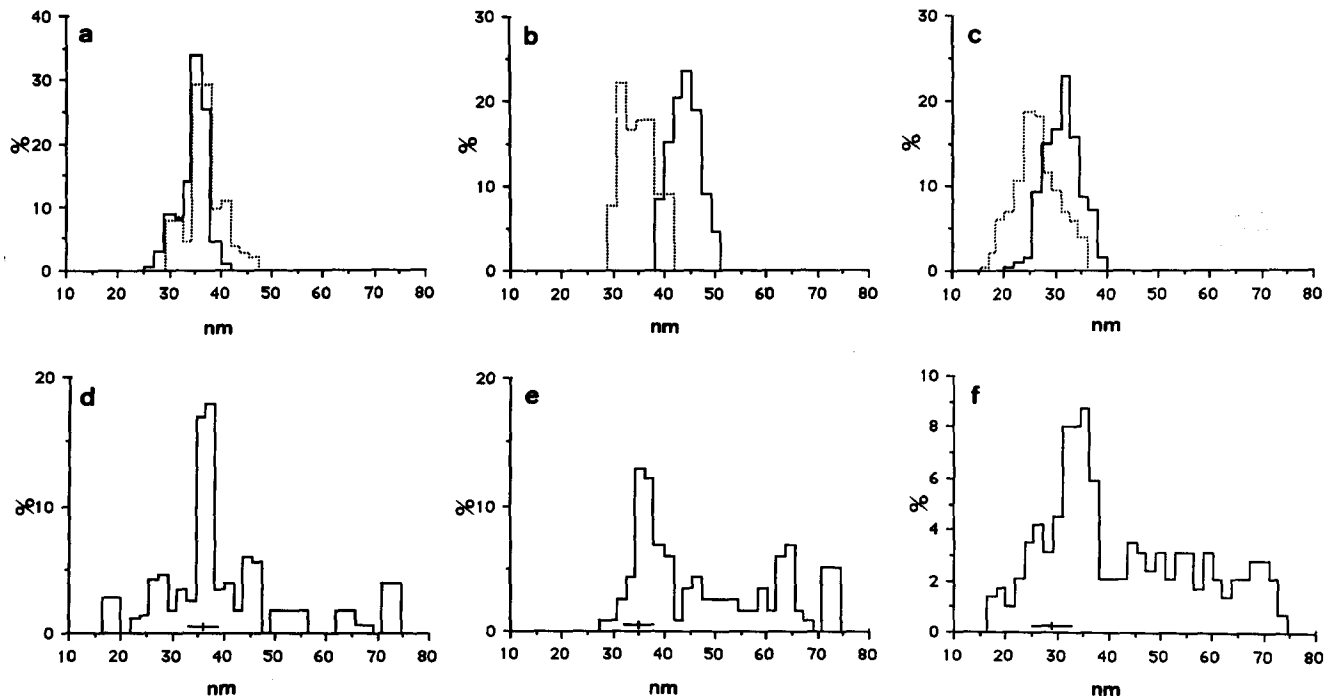

Figure 8. Histograms representing the distributions of molecular lengths and minimal longitudinal spacings along actin filaments of the different α-actinin isoforms. (*a–c*) Molecular lengths of free (*solid lines*) and F-actin-bound (*dotted lines*) α-actinin molecules. (*d–f*) Minimal longitudinal spacings of α-actinin molecules bound along actin filaments. The mean length and standard deviation of the bound α-actinin molecules (see Table I) are marked in the three histograms (*d–f*). (*a* and *d*) Chicken gizzard; (*b* and *e*) *Acanthamoeba*; and (*c* and *f*) *Dictyostelium* α-actinin.

Contrary to what has been reported by Condeelis and Vahey (1982), the *Dictyostelium* α-actinin used by us, which we are confident was intact since morphologically its interaction with F-actin was indistinguishable from that of the other two isoforms (see above paragraph on Apparent α-Actinin-F-Actin Dissociation Constants), was unable to induce significant F-actin bundle formation under experimental conditions where bundles readily formed with the other two α-actinin isoforms. Most likely, this discrepancy is due to subtle differences in the respective bundling assays used.

Relative Orientation of Actin Filaments Cross-linked by α-Actinin

We used the vorticity of axial projections computed from filament 3-D reconstructions as a criterion to evaluate the relative orientations of cross-linked actin filaments both within ladder-like α-actinin-F-actin bundles as well as in F-actin networks. While the relative polarities were different for different α-actinin isoforms, in no case were they random but revealed a clear trend for each isoform, i.e., antiparallel for smooth muscle and *Dictyostelium* α-actinin, and parallel for *Acanthamoeba* α-actinin (Table I). Our polarity analysis, however, has not yielded a correlation between the F-actin bundling potential of a particular α-actinin isoform and the relative polarity of the actin filaments cross-linked by this isoform.

The Length of the α-Actinin Molecule Determines Its F-Actin Bundling Potential

Most of the published length values of α-actinin molecules have been measured from either quick-frozen/deep-etched material (Pollard et al., 1986), or glycerol-sprayed/rotary metal-shadowed preparations (Condeelis and Vahey, 1982; Condeelis et al., 1984; Wallraff et al., 1986). Only *Dictyostelium* α-actinin has been systematically evaluated from negatively stained material (Condeelis and Vahey, 1982). For chicken gizzard and *Acanthamoeba* α-actinin our measurements of glycerol-sprayed and rotary metal-shadowed

molecules are within one standard deviation of the published values. However, for *Dictyostelium* α-actinin our mean length significantly differs from that published by Condeelis and Vahey (1982) on the one hand, and from that by Wallraff et al. (1986) on the other. Condeelis and Vahey (1982) got 38.0 ± 4.9 nm, compared with 31.4 ± 3.4 nm measured by us on negatively stained preparations. An even larger difference exists for glycerol-sprayed/rotary metal-shadowed preparations, for which we have measured a mean length of 34.3 ± 4.5 nm compared with 55.7 nm obtained by Wallraff et al. (1986). In view of these apparent discrepancies, it is important to note that in our case all three α-actinin isoforms were prepared in exactly the same way for electron microscopy, thus allowing for a rigorous comparison. Therefore, we feel that while the mean lengths we have determined for the different α-actinin isoforms may not necessarily represent their absolute values, the relative length differences are likely to be significant since they are based upon common preparation and evaluation protocols.

We have found that the mean length of both *Acanthamoeba* as well as *Dictyostelium* α-actinin significantly shortens upon binding to actin filaments. This shortening is most prominent with *Acanthamoeba* (i.e., from 44.1 to 35.0 nm), less obvious with *Dictyostelium* (i.e., from 31.4 to 28.1 nm), and practically absent with chicken gizzard (i.e., from 34.8 to 36.1 nm) α-actinin. Accordingly, the two α-actinin isoforms with F-actin bundling potential (i.e., chicken gizzard and *Acanthamoeba*) assume a molecular length similar to the F-actin helical repeat (i.e., 35.8 nm) upon binding to actin filaments. Among the possible explanations for these length changes occurring between free and bound α-actinin molecules are: (*a*) an "elastic" rod or head domain, (*b*) the ability of the two rod domains within the homodimer to "glide" by some amount relative to each other, or (*c*) a conformational change taking place within the "knob-like" NH_2-terminal actin-binding domain. In fact, a shortening of *Dictyostelium* α-actinin upon binding of certain monoclonal antibodies to the molecule has also been reported (Wallraff et al., 1986). It will be interesting to see, whether spectrin and dystrophin,
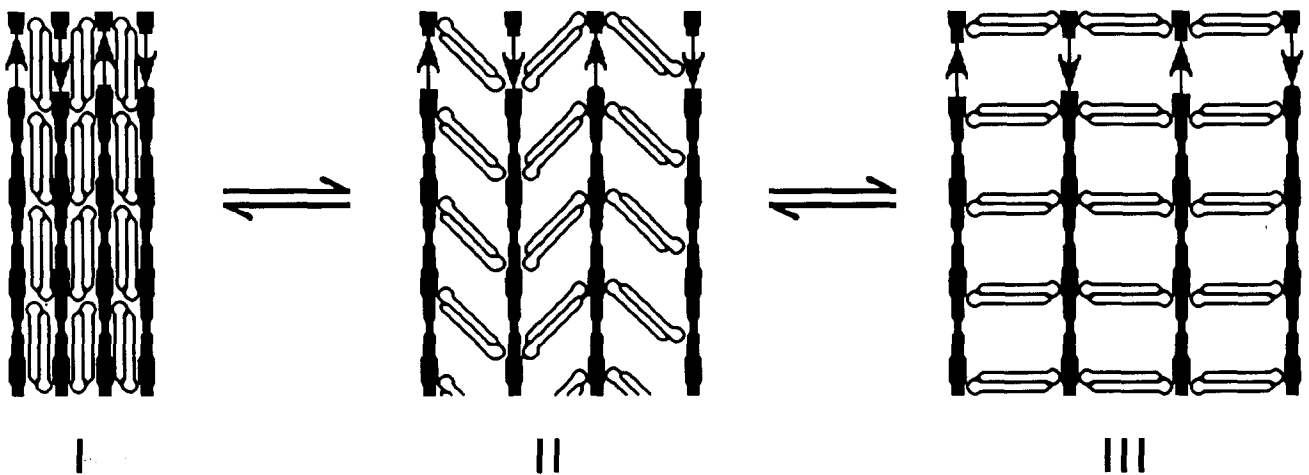

Figure 9. "Dynamic" model of α-actinin-F-actin bundles which allows "switching" between "tight" bundles (*I*) and "loose" bundles (*III*). In tight bundles all α-actinin molecules are oriented with their long axis parallel to the actin filament axis. In loose bundles all α-actinin molecules have switched from a parallel to a perpendicular orientation relative to the actin filaments, probably via obliquely oriented intermediates (*II*).

which, together with α-actinin, comprise the spectrin super-family (Byers et al., 1989), are elastic too and may change their length upon interaction with actin filaments.

We also measured the minimal longitudinal spacings between α-actinin molecules bound along the length of actin filaments within ladder-like α-actinin–F-actin complexes. With all three isoforms, the majority of longitudinal spacings was always larger than the respective mean molecular length of the bound α-actinin isoform under investigation (see mean length marks in Fig. 8, d–f). For the two α-actinin isoforms having F-actin bundling potential (i.e., chicken gizzard and Acanthamoeba α-actinin) the minimal significant longitudinal spacing (Fig. 8, d and e) roughly coincided with the length of the molecule, and hence with the F-actin helical repeat (i.e., 35.8 nm), suggesting that the length of the bound α-actinin molecule determines its minimal longitudinal spacing along the actin filaments. This length constraint, in turn, ensures that all the α-actinin molecules within tight α-actinin–F-actin bundles, as they form in solution with saturating α-actinin to actin molar ratios, are oriented with their long axis parallel to the actin filament axes (Fig. 9 I) rather than twisting around the filaments. In this configuration, tight bundles may be converted into loose bundles (i.e., by lowering the surrounding pool of free α-actinin) where the α-actinin molecules "switch" from a parallel to a near perpendicular orientation (Fig. 9 III), probably via obliquely oriented intermediates (Fig. 9 II). As illustrated schematically in Fig. 9, the different α-actinin–F-actin configurations of this dynamic process may be "trapped" by chemical fixation. In this model, the much shorter Dictyostelium α-actinin, and hence the concomitant shorter longitudinal spacing along the actin filaments, perturbs F-actin bundling.

The biological significance of actin filament bundle formation by α-actinin remains elusive. However, a significant evolutionary pressure must have conserved the length of the α-actinin molecule when bound to actin filaments, as a protozoan α-actinin (Acanthamoeba) has the same molecular length than a vertebrate α-actinin (chicken gizzard) which, in addition, coincides with the length of the F-actin helical repeat. Therefore, it is likely that α-actinin has an important role in focal contact as well as in stress fiber formation and, indeed, most of the α-actinin in nonmuscle cells accumulates there (Lazarides and Burridge, 1975).

Note Added in Proof. According to Demma et al. (Demma, M., V. Warren, R. Hock, S. Dharmawardhane, and J. Condeelis 1990. Isolation of an abundant 50,000-dalton actin filament bundling protein from Dictyostelium amoeba. J. Biol. Chem. 265:2286–2291), the only two actin binding proteins of all those described so far in Dictyostelium ameba that bundle actin filaments in vitro are a 30- and a 50-kD protein, implying that Dictyostelium α-actinin, in agreement with our finding, does not bundle actin filaments in vitro.

References

Aebi, U., R. Milloning, H. Salvo, and A. Engel. 1986. The three-dimensional structure of the actin filament revisited. Ann. NY Acad. Sci. 483:100–119.

Baron, D. B., M. D. Davison, P. Jones, and D. R. Critchley. 1987. The sequence of chick α-actinin reveals homologies to spectrin and calmodulin. J. Biol. Chem. 262:17623–17629.

Blanchard, A., V. Ohanian, and D. Critchley. 1989. The structure and function of α-actinin. J. Muscle Res. Cell. Motil. 10:280–289.

Buhle, E. L., U. Aebi, and P. R. Smith. 1985. Correlation of surface topography of metal-shadowed specimens with their negatively stained reconstructions. Ultramicroscopy. 16:436–450.

Burn, P., A. Rotman, R. K. Meyer, and M. M. Burger. 1985. Diacylglycerol in large α-actinin/actin complexes and in the cytoskeleton of activated platelets. Nature (Lond.). 314:469–472.

Burridge, K., and J. R. Feramisco. 1981. Nonmuscle α-actinins are calcium-sensitive actin binding proteins. Nature (Lond.). 294:565–567.

Byers, T. J., A. Husain-Chishti, R. R. Dubreuil, D. Branton, and L. S. B. Goldstein. 1989. Sequence similarity of the amino-terminal domain of Drosophila beta spectrin to α-actinin and dystrophin. J. Cell Biol. 109:1633–1641.

Condeelis, J. S., and M. Vahey. 1982. A calcium- and pH-regulated protein from Dictyostelium discoideum that cross-links actin filaments. J. Cell Biol. 94:466–471.

Condeelis, J. S., M. Vahey, J. M. Carboni, J. DeMey, and S. Ogihara. 1984. Properties of the 120,000- and 95,000-dalton actin-binding proteins from Dictyostelium discoideum and their possible function in assembling the cytoplasmic matrix. J. Cell Biol. 99(1, Pt. 2):119s–126s.

Cooper, J. A. 1987. Effects of cytochalasin and phalloidin on actin. J. Cell Biol. 105:1473–1478.

Duhaiman, A. S., and J. R. Bamburg. 1984. Isolation of brain α-actinin. Its characterization and comparison of its properties with those of muscle α-actinins. Biochemistry. 23:1600–1608.

Ebashi, S., F. Ebashi, and K. Maruyama. 1964. A new protein factor promoting contraction of actomyosin. Nature (Lond.). 203:645–646.

Endo, T., and T. Masaki. 1982. Molecular properties and functions in vitro of chicken smooth-muscle α-actinin in comparison with those of striated-muscle α-actinins. J. Biochem. 92:1457–1468.

Engel, A., and R. Reichelt. 1989. Scanned and fixed beam microscopy of cytoskeletal components. In Cytoskeletal and Extracellular Proteins, Structure, Interactions and Assembly. The 2nd International EBSA (European Biophysical Societies Association) Symposium. U. Aebi and J. Engel, editors. Springer-Verlag, Berlin. 187–202.

Feramisco, J. R., and K. Burridge. 1980. A rapid purification of α-actinin filamin and a 13,000-dalton protein from smooth muscle. J. Biol. Chem. 255:1194–1199.

Fowler, W. E., and U. Aebi. 1983. Preparation of single molecules and supramolecular complexes for high-resolution metal shadowing. J. Ultrastruct. Res. 83:319–334.

Goll, D. E., A. Suzuki, J. Temple, and G. R. Holmes. 1972. Studies on purified α-actinin. I. Effect of temperature and tropomyosin on the α-actinin/F-actin interaction. J. Mol. Biol. 67:469–488.

Holmes, G. R., D. E. Goll, and A. Suzuki. 1971. Effect of α-actinin on actin viscosity. Biochim. Biophys. Acta. 253:240–253.

Imamura, M., T. Endo, M. Kurada, T. Tanaka, and T. Masaki. 1988. Substructure and higher structure of chicken smooth muscle α-actinin molecule. J. Biol. Chem. 263:7800–7805.

Isenberg, G., U. Aebi, and T. D. Pollard. 1980. An actin-binding protein from Acanthamoeba regulates actin filament polymerization and interactions. Nature (Lond.). 288:455–459.

Jockusch, B. M., and G. Isenberg. 1981. Interaction of α-actinin and vinculin with actin: opposite effects on filament network formation. Proc. Natl. Acad. Sci. USA. 78:3005–3009.

Lazarides, E., and K. Burridge. 1975. α-Actinin: immunofluorescent localization of a muscle structural protein in nonmuscle cells. Cell. 6:289–298.

Light, K. E. 1984. Analyzing nonlinear scatchard plots. Science (Wash. DC). 223:76–77.

Millonig, R., H. Salvo, and U. Aebi. 1988. Probing actin polymerization by intramolecular cross-linking. J. Cell Biol. 106:785–796.

Mimura, N., and A. Asano. 1987. Further characterization of a conserved actin-binding 27-kDa fragment of actinogelin and α-actinins and mapping of their binding sites on the actin molecule by chemical cross-linking. J. Biol. Chem. 262:4717–4723.

Mische, S. M., M. S. Mooseker, and J. S. Morrow. 1987. Erythrocyte adducin: a calmodulin-regulated actin bundling protein that stimulates spectrin actin binding. J. Cell Biol. 105:2837–2845.

Noegel, A., W. Witke, and M. Schleicher. 1987. Calcium-sensitive non-muscle α-actinin contains EF-hand structures and highly conserved regions. FEBS (Fed. Eur. Biochem. Soc.) Lett. 221:391–396.

Podlubnaya, Z. A., L. A. Tskhovrebova, M. M. Zaalishvili and G. A. Stefanenko. 1975. Electron microscopic study of α-actinin. J. Mol. Biol. 92:357–359.

Pollard, T. D. 1981. Purification of a calcium-sensitive actin gelation protein from Acanthamoeba. J. Biol. Chem. 256:7666–7670.

Pollard, T. D., P. C.-H. Tseng, D. L. Rimm, D. P. Bichell, R. C. Williams, Jr., J. Sinard, and M. Sato. 1986. Characterization of alpha-actinin from *Acanthamoeba*. *Cell Motil. Cytoskel*. 6:649–661.

Sato, M., W. H. Schwarz, and T. D. Pollard. 1987. Dependence of the mechanical properties of actin/α-actinin gels on deformation rate. *Nature (Lond.)*. 325:828–830.

Schleicher, M., G. Gerisch, and G. Isenberg. 1984. New actin-binding proteins from *Dictyostelium discoideum. EMBO (Eur. Mol. Biol. Organ) J.* 3:2095–2100.

Suzuki, A., D. E. Goll, I. Singh, R. E. Allen, R. M. Robson, and M. H. Stromer. 1976. Some properties of purified skeletal muscle α-actinin. *J. Biol. Chem.* 251:6860–6870.

Wallraff, E., M. Schleicher, M. Modersitzki, D. Rieger, G. Isenberg, and G. Gerisch. 1986. Selection of *Dictyostelium* mutants defective in cytoskeletal proteins: use of an antibody that binds to the ends of α-actinin rods. *EMBO (Eur. Mol. Biol. Organ.) J.* 5:61–67.

Wrigley, N. 1968. The lattice spacing of crystalline catalase as an internal standard of length in electron microscopy. *J. Ultrastruct. Res.* 24:454–464.